J Appl Electrochem (2011) 41:873–879
DOI 10.1007/s10800-011-0308-x

ORIGINAL PAPER

Improvement of passivity of Fe–*x*Cr Alloys ($x < 10\%$) by cycling through the reactivation potential

Jaganathan Ulaganathan · Nick A. Senior · Roger C. Newman

Received: 25 January 2011 / Accepted: 25 March 2011 / Published online: 7 April 2011

Abstract Classically, 13% Cr is required for stable passivity of a Fe–Cr alloy in acidic and neutral solutions not containing inhibitors. Some authors (Mansfeld, Fujimoto) have published potential cycling procedures that generate thick Cr-rich films. In this work, a similar technique, but with a far smaller potential cycle, was used to enrich a surface layer in chromium, thereby increasing corrosion-resistance in otherwise non-passivating steels. This was achieved by potential stepping across the iron reactivation potential, firstly forming passive iron(III) oxide, then reducing it to soluble iron(II) ions, while ensuring the passivity of chromium. The use of potential stepping was found to result in a more robust film than that formed through a single continuous passivation step.

Keywords Iron–chromium alloy · Passivity · Potential cycling · Reactivation potential

1 Introduction

Classically, stainless steels (Fe–[Ni]–Cr alloys) require a minimum of 13 at% chromium in order to form a stable Cr-enriched passive layer in mildly acidic media (pH < 4). This barrier film prevents continued iron dissolution, and the Cr enrichment is due to the preferential dissolution of Fe and/or reductive dissolution of iron(III) oxide [1–5], and the low mobility and high stability of Cr cations in the passive film [2, 6, 7].

J. Ulaganathan · N. A. Senior · R. C. Newman (✉)
Department of Chemical Engineering and Applied Chemistry, University of Toronto, 200 College Street, Toronto, ON M5S 3E5, Canada
e-mail: roger.newman@utoronto.ca

Below the 13 at% threshold, alloys are susceptible to corrosion, as the Cr content is insufficient to attain complete coverage on the surface by Cr oxide. The resulting film can be porous, through which iron can dissolve. If, instead, environmental conditions permit the enrichment of chromium without continuous porosity formation, passivity can be conferred to the steel. The degree of Cr enrichment in the surface film has been shown to be higher in alloys with lower Cr content by Kirchheim et al. [2], who analyzed Fe–Cr alloys with Cr content ranging from 0.6 to 18 at%. In this study, we explore a potential cycling method to form thicker and more continuous Cr-rich oxide (or oxyhydroxide) films on low-Cr alloys.

In earlier work, Mansfeld, Fujimoto and others established potential cycling methods to form thicker passive films on stainless steel. Mansfeld [8] was interested in surface modification without involving chemically hazardous baths like those involving Cr^{6+} ions. Fujimoto [9] was interested in forming thick, coloured passive films. In both studies, the potential was applied as a square wave, stepping between two potentials at chosen frequencies. Fujimoto et al. observed a linear film growth when the lower potential, E_A, and the higher potential, E_P, corresponded with the active and passive regions of chromium. The linear growth was attributed to the formation of Cr^{3+} oxides from Cr^{2+} ions in solution at E_P, with replenishment of Cr^{2+} ions by anodic dissolution of Cr at E_A. In a second set of experiments, the potentials were chosen from the passive (E_P) and trans-passive (E_{TP}) regions of chromium. Under these circumstances, linear film growth occurred through cathodic reduction of Cr^{6+} ions at E_P, whilst Cr^{6+} ions were formed by trans-passive dissolution at E_{TP}.

In this study, the enrichment in chromium comes about through the selective dissolution of Fe from and through iron(III) oxides, as the applied potential alternates between

the passive (E_P) and active (E_A) regions of iron. It is well known that iron is reactivated from the passive state (by reductive dissolution of iron(III) oxides) below the 'Umschlagspunkt', the so-called Flade potential or reactivation potential [10]. The electrochemical conditions were chosen such that at all potentials, chromium itself remained passive (see super-imposed Pourbaix diagram for details, Fig. 1). This permitted investigation into the possibility of continuous formation of chromium(III) oxides (or oxyhydroxides) on the surface with an intention to produce a stainless-steel-like surface on the low-Cr alloy.

According to a percolation model, by Newman and Sieradzki [11], passivity of Fe–Cr alloys can be explained as the formation of an infinite –Cr–O–Cr– polymeric oxide network on the surface. In order to form this network, the model requires the alloy to have a minimum of 9.5 at% Cr atoms in the bulk, where each Cr atom can form oxygen bridges with its first, second and third nearest neighbouring Cr atoms. If only the first and second nearest-neighbouring Cr atoms are available to form the network, the alloy requires >17.5 at% Cr [12, 13]. The classical 13 at% threshold is viewed as a reactivation threshold by this percolation model, i.e., the underlying metal would be reactivated from its passive state below a 13 at% Cr content in the original alloy, but not above [14]. This view was modified recently [15] with the realization that slow dissolution does continue between 13 and 17.5 at% Cr, but the rate is so slow it can hardly be distinguished from the passive state.

In the case of low-Cr alloys, at the instance of applying a passivation potential, a pseudo-steady state is reached with the formation of chromium(III) oxide (or oxyhydroxide). The lack of sufficient Cr content in the alloy results in discontinuity in the –Cr–O–Cr– network. Under a constant passivation potential, where iron(III) oxide (or oxyhydroxides) are formed, the chromium oxide is prevented from forming the infinite network. By stepping the potential to a region where removal of the surface iron(III) oxides is selectively enabled (E_A according to the potential stepping method described earlier), fresh Cr atoms in the lattice can be exposed, with which existing –Cr–O–Cr– clusters with hydroxide terminations can bond, resulting in a more robust Cr-rich, and perhaps passivating film.

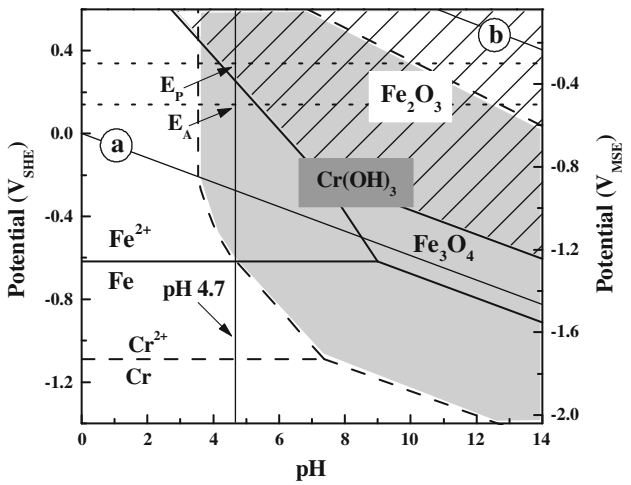

Fig. 1 Superimposed potential—pH diagram for the systems iron–water (*solid line*) and chromium–water (*dashed line*) at 25 °C, with stability regions for Fe_2O_3 (*area with upper right to lower left fill*) and $Cr(OH)_3$ (*grey area*) highlighted (*Equilibrium lines* have been constructed for the depicted potential range using respective equations from [17])

2 Experimental procedures

Fe–8 at% Cr and Fe–10 at% Cr sheets (from now on, Fe–8Cr; Fe–10Cr) were used in this study. Samples were cut from the sheets as ~20 mm × ~5 mm strips and annealed at 950 °C for 50 min in Ar/2.5% H_2 (4 ppm O_2), followed by quenching in de-ionised water. The samples were then mounted in epoxy with the cross-section exposed. They were polished to 1,200 grit finish immediately prior to immersion in the electrolyte. An equimolar acetic acid/sodium acetate (0.05 M/0.05 M) solution, deoxygenated by N_2 gas (99.998%, $O_2 < 3$ ppm), was used as the electrolyte, at 22 ± 2 °C. AnalaR® grade glacial acetic acid, CH_3COOH (99.8%) and ACS grade sodium acetate tri-hydrate, $CH_3COONa.3H_2O$ (99%) were used to prepare the buffer solution. The solution had a pH of 4.7, close to its pK_a value of 4.75, and was considered sufficiently dilute to neglect complexation effects.

In the electrochemical experiments, potentials were measured with a saturated mercury-mercurous sulphate electrode (MSE). A platinum wire was used as counter electrode. DC electrochemical studies were carried out using a software-controlled Gamry Femtostat™ system. Prior to each experiment, the samples were cathodically pre-treated at −1.4 V_{MSE} for 60 s, to remove air formed oxide film. For the potential cycling experiments, the potential was applied in the form of a square wave by stepping between iron passivation (E_P) and activation (E_A) potentials for a fixed number of cycles. One passivation and subsequent activation step is one cycle.

In a few of the figures, data are also shown for pure Fe, from an earlier publication on the reactivation of that metal in the same electrolyte [16].

3 Results and discussion

The activation potential (E_A) for potential cycling, can be chosen from a wide range of potential between iron

immunity and passivation (−1.24 to −0.4 V_{MSE}, at pH 4.7). Cr remains passive in the entirety of this region (Fig. 1). To be sure of reducing an already-formed iron passive film, it is important to determine the reactivation potential of iron as it signals the onset of loss of iron(III) oxides by reductive dissolution. One should not confuse the terminologies—'activation' and 'reactivation'. Reactivation is a phenomenon by which the metal or alloy loses its passivity and undergoes anodic dissolution from the exposed surface, when polarized below a specific reactivation potential.

Several methods have been described in the literature to determine the reactivation potential. According to Davenport et al. [14], Fe–Cr alloys are reactivated when the open circuit potential of the passivated surface drops to a value where iron(III) oxides undergo reductive dissolution to iron(II) ions, resulting in activation of the exposed surface. Kirchheim et al. [2] define it as the potential at which the current density reaches mid-value between passive and active states, during back-scanning from the passive state. In this study, the reactivation potential is defined at the minimum in current density during back-scanning of the potential from the passive state.

The reactivation of iron from its passive state is demonstrated in Fig. 2. Pure elemental Fe was subjected to passivation at −0.3 V_{MSE} for 30 min, followed by a reverse potential scan at 0.1 mV s^{-1}. The reactivation potential was identified, from the current minimum, as −0.375 V_{MSE}. The E_A for the potential cycling procedure, to facilitate Cr enrichment in low-Cr alloys, is always chosen below this iron reactivation potential. In addition, alloy composition is anticipated to significantly affect the reactivation potential and thereby the Cr enrichment. With this in mind, Fe–8Cr and Fe–10Cr were subjected to reactivation under the same conditions as elemental Fe. The results are presented along with that of Fe in Fig. 2, and demonstrate that the rate of dissolution from the reactivated surface decreases with an increase in Cr content. However, both Fe–8Cr and Fe–10Cr are reactivated at the same potential, and below the iron reactivation potential.

The baseline electrochemical behaviour of Fe–8Cr, in pH 4.7 acetate buffer, is shown in Fig. 3. The active–passive transition and passive behaviour are clearly evident from the anodic polarization, from which −0.3 V_{MSE}, at the start of the passive region, was chosen as E_P for the potential cycling. The Pourbaix diagram (Fig. 1) verifies that both Fe and Cr should passivate at this potential.

Figure 4 demonstrates the scan rate dependence of the reactivation of Fe–8Cr from the passive state, in acetate buffer. This indicates that the reductive dissolution of the passive film is time-dependent (and more so than that of pure Fe), i.e., sufficient time should be spent at the reactivation potential to completely remove the passive film

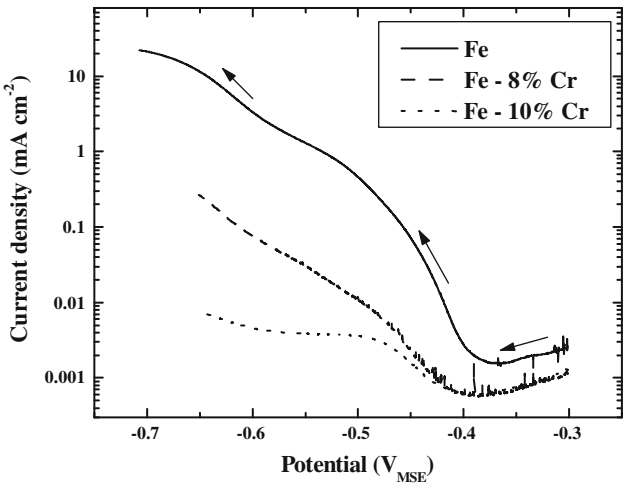

Fig. 2 Reactivation of Fe, Fe–8Cr, and Fe–10Cr in pH 4.7 acetate buffer by potential back-scanning at 0.1 mV s^{-1} from the passive state formed by passivation at −0.3 V_{MSE} for 30 min

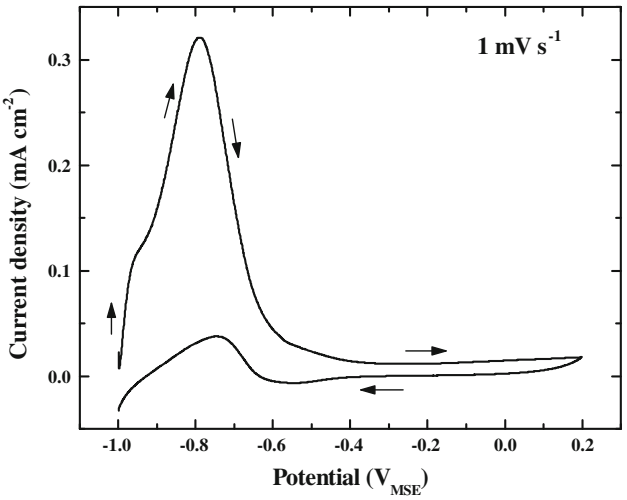

Fig. 3 Potentiodynamic polarization of Fe–8Cr in pH 4.7 acetate buffer at a scan rate of 1 mV s^{-1}

and expose the bare surface for further dissolution. Hence, a reduced peak current density is observed at faster scan rates, due to contributions from reductive dissolution of the remnant passive film. Therefore, the rate of anodic dissolution on the reactivated surface was measured at steady state, following potential steps from the passive state, and is shown in Fig. 5. The approximate reactivation potential (E_R) of Fe–8Cr was identified, by the current minimum, as −0.50 V_{MSE}, and was used as E_A for potential cycling. This E_A is below the iron reactivation potential (−0.375 V_{MSE}) ensuring removal of iron(III) oxides by reductive dissolution during potential cycling. It is to be noted that cathodic current densities were not obtained, in contrast to potentiodynamic back-scans at faster scan rates. This is due to the incomplete removal of the passive film at faster scan

rates, and the reduction of the film itself contributing to the observed cathodic currents.

Fe–8Cr specimens were then passivated with and without potential cycling. During potential cycling the specimen was subjected alternatively to passivation ($E_P = -0.3$ V_{MSE} for 30 min) and activation ($E_A = -0.5$ V_{MSE} for 3 min) for 5 cycles. After the 5 cycles, a passive film was formed on the specimen at -0.3 V_{MSE} for 30 min. In total, the specimen was exposed to the acetate buffer for 195 min (Fig. 6). For direct comparison, the samples passivated with and without potential cycling were exposed to the passivating environment for the same duration. Therefore on the specimen not subjected to potential cycling, the passive film was formed at -0.3 V_{MSE} for 195 min (Fig. 7). This was done to eliminate the possibility that the differences that arise might be because of the thicker passive film formed from longer exposure. These procedures for preparing passive films are hereafter referred to as the 'standard' method.

The effectiveness of the passive films thus formed was determined by measuring dissolution rates on the reactivated surfaces. This was done by scanning the applied potential backwards from the passivation potential (Fig. 8). The potential was scanned at a rate of 0.1 mV s^{-1}, which was considered sufficiently slow to assume equivalence to steady state. Whilst both electrodes produced similar current trends, the current was considerably lower for the specimen passivated with potential cycling.

Our interpretation is that when the passive film is formed in one step, the –Cr–O–Cr– network is formed only in small disconnected clusters due to the insufficient Cr content in the bulk. When the iron(III) oxides (or oxyhydroxides) are lost by reductive dissolution during reactivation, portions of chromium(III) oxide (or oxyhydroxides)

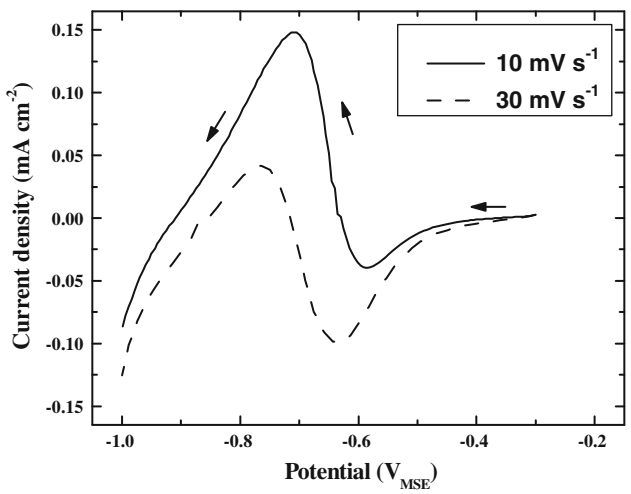

Fig. 4 Reactivation of Fe–8Cr in pH 4.7 acetate buffer by potential back-scanning at 10 and 30 mV s^{-1} from the passive state formed by passivation at -0.3 V_{MSE} for 30 min

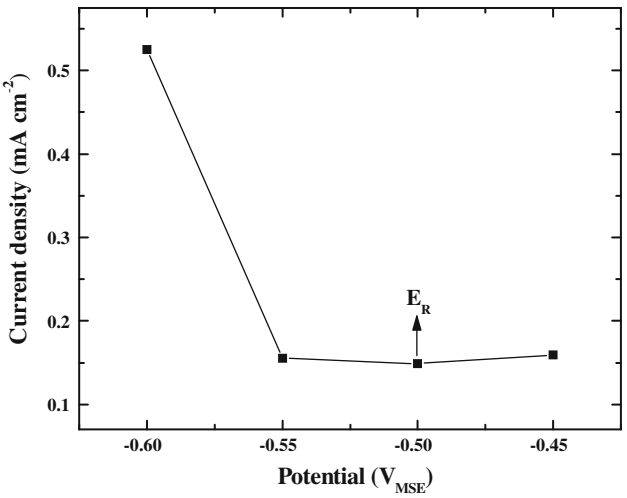

Fig. 5 Reactivation current densities on Fe–8Cr in pH 4.7 acetate buffer measured potentiostatically after 30 min, following potential steps from the passive state formed by passivation at -0.3 V_{MSE} for 30 min

clusters that were embedded within the iron(III) oxides (or oxyhydroxides) can detach, thereby increasing the effective surface area[1] available for anodic dissolution, at least temporarily. The detachment of finite clusters has been evidenced from discrepancies between weight loss measurements and the anodic charge passed on Fe–Cr alloys with varying Cr content and polarized in the partial passivation region in a single step [12]. Forming the passive film with potential cycling improves the connectivity of the –Cr–O–Cr– network, thereby reducing the effective surface area available for dissolution. This is evidenced from the inset graph in Fig. 6. When stepping to E_A, the current always shows a transition from cathodic to anodic character implying the initial reduction of connected iron(III) oxides followed by subsequent iron dissolution and chromium passivation from the exposed surface area. The improved connectivity in the –Cr–O–Cr– network is also evidenced from the decrease in passivation current densities with subsequent passivation steps in the potential cycling procedure (Fig. 6). This tendency of the passive film to lower the passivation current density diminishes and saturates with an increase in number of cycles, as was observed from 10 cycles of potential cycling (data not shown). This involves extended exposure to the passivating environment during potential cycling and so cannot be directly compared to the 'standard' passive film formed without potential cycling shown in Fig. 8, unless it is formed for the same extended duration.

As described earlier, the E_A value of -0.5 V_{MSE} corresponded with the reactivation potential of Fe–8Cr,

[1] The current density recorded in Fig. 8 is relative to the initial surface area.

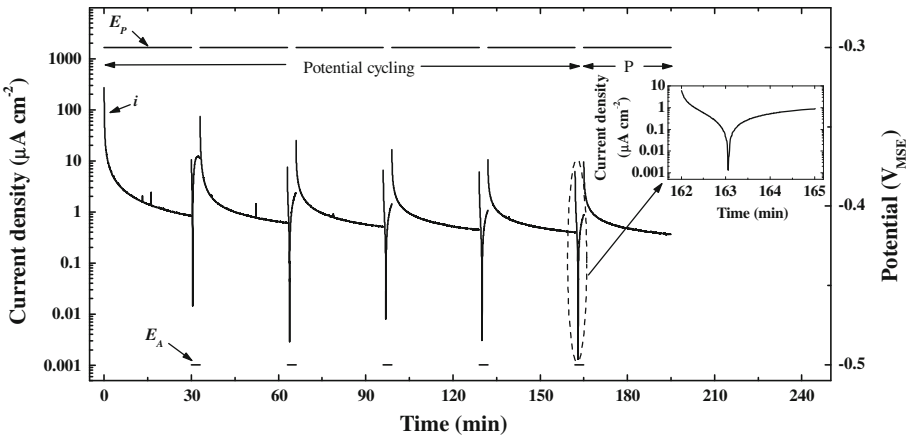

Fig. 6 Standard method for passivation of Fe–8Cr in acetate with potential cycling (5 cycles with $E_P = -0.3$ V_{MSE} for 30 min and $E_A = -0.5$ V_{MSE} for 3 min). The potential cycling is concluded with passivation at -0.3 V_{MSE} for 30 min. *Inset graph* shows one activation step in detail

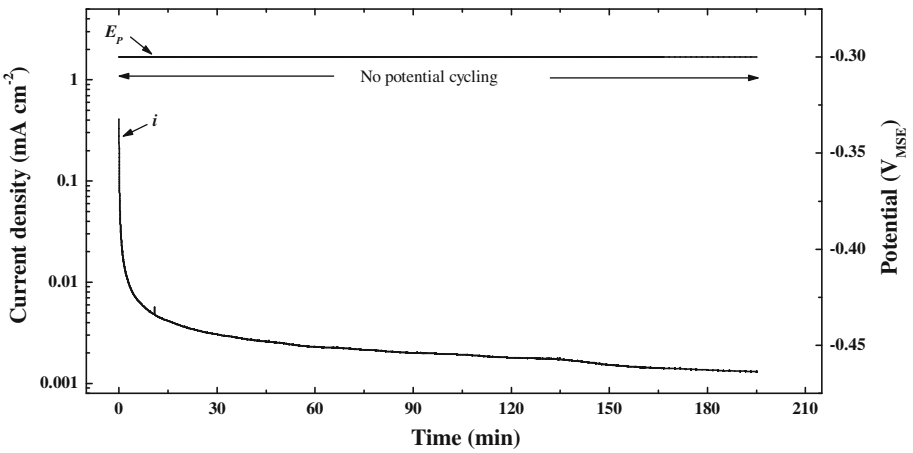

Fig. 7 Standard method for passivation of Fe–8Cr in pH 4.7 acetate buffer without potential cycling, at -0.3 V_{MSE} for 195 min

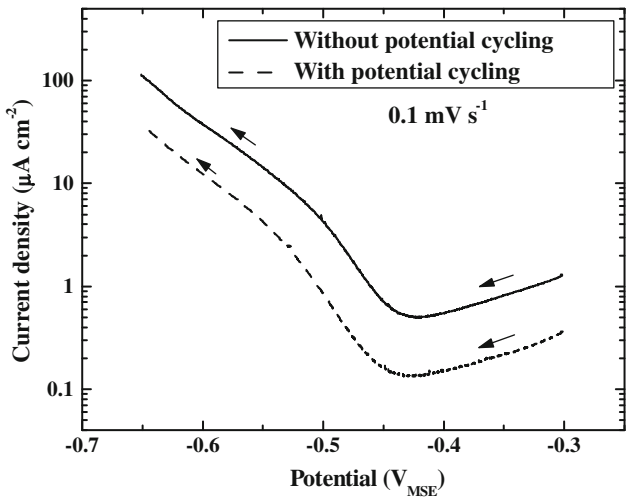

Fig. 8 Reactivation of Fe–8Cr in pH 4.7 acetate buffer by potential back-scanning at 0.1 mV s^{-1} from passive state formed using the 'standard' method with potential cycling (5 cycles, $E_A = -0.5$ V_{MSE}) and without potential cycling

although, as iron is active over a range of potentials, other values of E_A could also be used. Indeed, E_A provides a means of altering the structure of the porous film formed by controlling the balance between iron(III) reduction, iron(II) dissolution, and surface chromium oxidation that hinders the propagation of porosity. Therefore, the potential cycling behaviour of Fe–8Cr was further studied with two more E_A values, one cathodic and one anodic to the reactivation potential of Fe–8Cr, but both more negative than that of pure Fe. The intent was to investigate the sensitivity of E_A on the rate of iron(III) oxide reduction, and consequently on iron dissolution and chromium oxidation from the exposed surface.

The 'standard' passive film procedure was thus repeated using the three E_A potentials of -0.4, -0.5, and -0.6 V_{MSE}. Following the final passivation phase, samples were polarized to either -0.4, -0.5 or -0.6 V_{MSE}, in contrast to the potential back-scan used previously. The current densities recorded following 1 h of polarization are presented in Fig. 9.

The data demonstrate that the higher the activation potential, E_A, (i.e. the smaller the overpotential for reductive iron(III) dissolution) the less effective is the passive film formed on the low-Cr alloy. Indeed, using an E_A value more positive than the Fe–8Cr reactivation potential, the protective capability of the final film was less than that

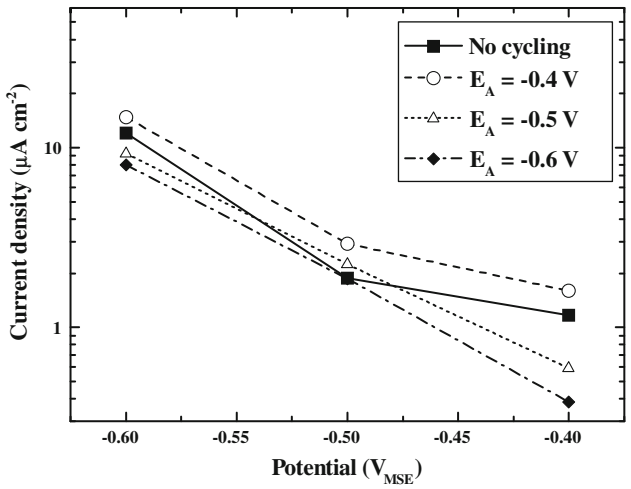

Fig. 9 Reactivation current densities of Fe–8Cr in pH 4.7 acetate buffer measured potentiostatically after 1 h, following potential steps to −0.4, −0.5, and −0.6 V_{MSE}, from the standard passive state formed with potential cycling (E_A = −0.4, −0.5, and −0.6 V_{MSE}) and without potential cycling

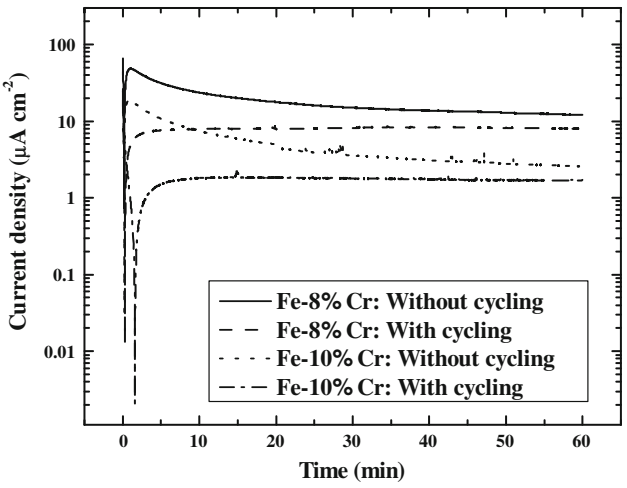

Fig. 10 Reactivation of Fe–8Cr and Fe–10Cr in pH 4.7 acetate buffer potentiostatically at −0.6 V_{MSE} (cathodic to the Fe–8Cr reactivation potential), from the standard passive state formed with potential cycling (E_A = −0.6 V_{MSE}) and without potential cycling

formed without cycling. These findings add credibility to the theory that more comprehensive the removal of the iron(III) oxide, which inhibits the formation of new chromium oxide, the greater the subsequent chromium enrichment.

For both the samples that did not undergo potential cycling and those with E_A = −0.4 V_{MSE}, Fig. 9 shows a change in slope above the Fe–Cr reactivation potential (but still below the Fe reactivation potential). It is possible that the Fe–Cr alloys do in fact reactivate at the same potential as pure Fe, but that this is an extremely slow process, or occurs only locally within the film.

The improvement in the resistance of Fe–8Cr to reactivation is not dramatic. This is demonstrated by the modest reductions in current density of the reactivated surface, averaging 24% for E_A = −0.5 V_{MSE}, and 34% for E_A = −0.6 V_{MSE} when compared to passive layers formed without potential cycling. However, this work demonstrates that an improvement in passive behaviour of chromium-deficient steels is technically feasible, and that optimisation of the potential cycling procedure would be anticipated to improve the results further. Modifications include the length of time spent at the activation and passivation potentials, and the number of cycles induced.

The effect of Cr content on potential cycling was investigated on Fe–8Cr and Fe–10Cr alloys via the 'standard' methodology, with E_A = −0.6 V_{MSE} (i.e., well cathodic to the reactivation potential of Fe–8Cr). Following passive film formation, the samples were potentiostatically held at −0.6 V_{MSE} for 1 h, in order to analyze the resistance shown by the passive film to reactivation (Fig. 10). It was observed that potential cycling improved the resistance to reactivation and anodic dissolution for both 8 and 10% Cr alloys, compared with films formed without potential cycling. Also the degree of resistance increased with the increase in Cr content. At steady state, the reactivation current density measured on Fe–10Cr was slightly less than one-fifth of that measured on Fe–8Cr, when both were subjected to potential cycling.

From this preliminary electrochemical study, a mechanism is proposed to explain the outcome of the potential cycling method and is illustrated in Fig. 11. During initial passivation, both iron(III) compounds (white regions) and chromium(III) compounds (black regions) are formed on the surface. On stepping to the activation potential, iron oxides are lost to solution as ferrous ions by reductive dissolution, but chromium oxide [for which read 'some combination of oxide and oxyhydroxide'] remains intact, with some disconnected clusters detaching. From the exposed surface, iron undergoes dissolution and chromium is oxidized. The fresh chromium oxide can either connect to existing chromium oxide clusters, enabling a kind of sol–gel transition, or can form separately. On stepping back to passivation potential, freshly exposed iron and chromium oxidize at the metal/film interface. Thus, stepping between the two potentials repeatedly would continually enrich the passive film in Cr and as well improve the −Cr–O–Cr– connectivity. The key component of this theory is the passive nature of chromium throughout the potential region utilized in potential cycling, chromium being known to passivate above a very negative potential of −0.6 V_{SHE} (−1.24 V_{MSE}) at pH 4.7, which is the pH of the acetate buffer used in this study [17].

Further study of the events occurring between the (apparent) reactivation potentials of pure Fe and the Fe–Cr

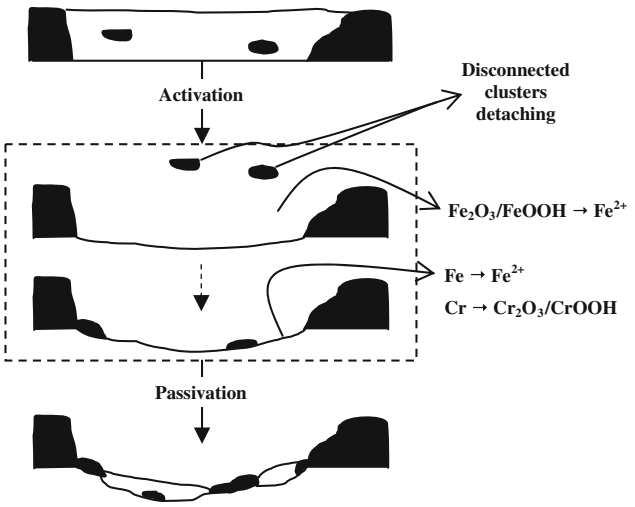

Fig. 11 Illustration of mechanism underlying the potential cycling with *white area* representing Fe_2O_3/FeOOH and *black area* representing Cr_2O_3/CrOOH

alloys would be beneficial for better understanding. Analysis of the surface by techniques such as XPS, and possibly in situ methods such as XANES, can provide quantitative information on the laterally averaged composition of a passive film formed by potential cycling, and even (in principle) the composition of the surface during reactivation. But such surfaces, and especially those where reactivation is in progress, are very sensitive to the atmosphere and even to rinsing. It would be beneficial to grow thicker passive films from longer potential cycling procedures to undertake meaningful studies of their composition and structure. The thickness of the passive film formed by the 'standard' potential cycling method in this study is estimated to be only 4 to 7 nm, assuming the passive film to be composed of iron(III) oxide/oxyhydroxide and Chromium(III) oxide/oxyhydroxide. Regarding the lateral variations, it is feasible that one could use some form of scanning probe microscopy that might be capable of capturing transitions from the initial gel-like structure of the passive film to a more condensed Cr-rich film.

4 Conclusions

In this work, potential cycling has been shown as an effective surface modification technique. The improvement in the passivation characteristics of low-Cr alloys after the application of the potential cycling method has been inferred mainly from two parameters—passivation current density, and resistance to reactivation from the passive state. Although this preliminary electrochemical work has been qualitative, the following conclusions can be drawn.

(1) The hypothesis that cycling of low-Cr alloys through the reactivation potential will continually enrich their passive films in Cr by selective dissolution of Fe holds true, based on reduction in anodic dissolution rates and resistance to reactivation.
(2) The activation potential, E_A, during potential cycling should be cathodic to the [apparent] reactivation potential of Fe–xCr ($x < 10\%$) alloy, as deleterious effects are clearly evident, while choosing an activation potential anodic to this potential. This is not fully understood yet, as pure Fe is reactivated at such E_A values.

Acknowledgements This research was supported by NSERC (Canada) and UNENE, the University Network of Excellence in Nuclear Engineering, via a Senior Industrial Research Chair awarded to R.C. Newman. Many thanks are due to A.G. Carcea for his assistance with the experiments.

References

1. Asami K, Hashimoto K, Shimodaira S (1978) Corros Sci 18:151
2. Kirchheim R, Heine B, Fischmeister H et al (1989) Corros Sci 29:899
3. Davenport AJ, Isaacs HS, Bardwell JA et al (1993) Corros Sci 35:19
4. Haupt S, Strehblow HH (1995) Corros Sci 37:43
5. Oblonsky LJ, Ryan MP, Isaacs HS (1998) J Electrochem Soc 145:1922
6. Kirchheim R, Heine B, Hofmann S et al (1990) Corros Sci 31:573
7. Maurice V, Yang WP, Marcus P (1996) J Electrochem Soc 143:1182
8. Kwiatkowski L, Mansfeld F (1993) J Electrochem Soc 140:L39
9. Fujimoto S, Shibata T, Wada K et al (1993) Corros Sci 35:147
10. Uhlig HH, King PF (1959) J Electrochem Soc 106:1
11. Sieradzki K, Newman RC (1986) J Electrochem Soc 133:1979
12. Newman RC, Meng FT, Sieradzki K (1988) Corros Sci 28:523
13. Qian S, Newman RC, Cottis RA et al (1990) J Electrochem Soc 137:435
14. Davenport AJ, Ryan MP, Simmonds MC et al (2001) J Electrochem Soc 148:B217
15. Smith GS, Newman RC, Fujimoto S et al (2010) J Electrochem Soc (submitted)
16. Ulaganathan J, Newman RC (2010) Electrochem Solid State Lett 13:C13
17. Pourbaix M (1974) Atlas of electrochemical equilibria in aqueous solution. NACE, Houston